

金属メッシュを利用したテラヘルツ帯 センシングの基礎検討

非会員 加藤 英志^{*,**}

非会員 吉田 永^{***}

非会員 林 伸一郎^{****,*****}

正員 小川 雄一^{**}

非会員 水津 光司^{**}

正員 川瀬 晃道^{**,****,*****}

The Basic Consideration of Sensing Method Using a Metallic Mesh in the Terahertz Range

Eiji Kato^{***}, Non-member, Hisa Yoshida^{***}, Non-member, Shin'ichiro Hayashi^{****,*****}, Non-member,

Yuichi Ogawa^{**}, Member, Koji Suizu, Non-member, Kodo Kawase^{****,*****}, Member

We report on a novel sensing method in the terahertz region using metallic mesh. Conventionally, the band-pass filter property of a metallic mesh can be adjusted by changing the mesh geometrical parameters. However, the band-pass filter parameters also depend on the refractive index of the medium in the vicinity of the mesh openings. To inspect this effect as a potential measurement principle, we calculated the electric field distribution around the metallic mesh and analyzed the frequency characteristics due to a sample attached to the metallic mesh using the Finite Difference Time Domain method. For bio-molecular sensing, the Electrospray Deposition method was applied in order to spray a uniform layer of protein over a metallic mesh. We observed a correlation between the quantity of protein and the transmission characteristics of the metallic mesh.

キーワード：テラヘルツ，金属メッシュ，表面プラズモンポラリトン，生体高分子センシング

Keywords : terahertz, metallic mesh, surface plasmon polariton, bio-molecular sensing

1. はじめに

テラヘルツ帯 (0.3 THz – 10 THz) と呼ばれる周波数帯では、実用に供する光源、検出器の開発がその他の周波数帯と比較して遅れていたため、未開拓の電磁波領域とされてきた。近年、小型卓上テラヘルツ光源⁽¹⁾に代表される光源技術や、テラヘルツ時間領域分光法 (Terahertz Time Domain Spectroscopy: THz-TDS)⁽²⁾に代表される計測技術が急速に進展し、テラヘルツ帯におけるアプリケーション開発が盛んに進められている。テラヘルツ波は、紙、プラスチック、

セラミック、木材、油脂などをある程度透過する電波の特性を有する最短波長の電磁波であり、かつ、レンズやミラーを用いて取回しが容易な光波としての最長波長の電磁波であるといえる。また、テラヘルツ帯ではさまざまな物質の特徴的なスペクトルが得られる領域でもあり、その対象は分子構造が比較的単純な気体、液体、固体などにおよぶ。そしてDNAに代表される生体高分子はそれらの結合状態により複素屈折率が異なるという知見が得られており⁽³⁾、バイオ応用が期待されている。さらに、テラヘルツ帯の波長は数百 μm のオーダーであり、実体顕微鏡に匹敵する空間分解能が得られ、イメージングによる非破壊検査応用が有望視されている⁽⁴⁾。

一方、金属の薄膜に正方形開口を規則的に配列した金属2次元周期構造 (金属メッシュ) は、1960年代にテラヘルツ帯において周波数選択性を有することが確認され、透過率が低い周波数領域では低損失のミラーや、ファブリペロー干渉計を構成する光学素子に応用されてきた⁽⁵⁾⁽⁶⁾。また、透過率が金属に対する開口の面積比よりも共鳴的に高くなる周波数領域⁽⁷⁾や、高透過率の周波数領域において入射条件により回折異常に起因する鋭いディップが現れることが知られている⁽⁸⁾。近年ではナノメートルオーダーのプロセス技術の

* (株) アドバンテスト研究所
〒989-3124 仙台市青葉区上愛子字松原 48-2

Advantest Labs. Ltd.,
48-2 Matsubara, Kamiyashiki, Aoba, Sendai 989-3124

** 名古屋大学大学院工学研究科
〒464-8603 名古屋市不老町
Graduate School of Nagoya Univ.,
Furo-cho, Nagoya 464-8603

*** 東北大学大学院農学研究科
〒981-8555 仙台市青葉区堤通雨宮町 1-1
Graduate School of Tohoku Univ.,

1-1 Amemiyamachi, Tsutsumidori, Aoba, Sendai 981-8555

**** 理化学研究所
〒980-0845 仙台市青葉区荒巻字青葉 519-1399
RIKEN,
519-1399 Aoba, Aramaki, Aoba, Sendai 980-0845

発達により光領域においても金属 2 次元周期構造が作成可能となり、同様な異常透過現象が報告されている⁽⁹⁾。本論文では、テラヘルツ帯において幅広く利用されている金属メッシュの諸特性の解析からセンシング応用への可能性を論じ、その検証として、たんばく質の微量検出を行い、高感度かつ簡便なセンシングへの応用可能性について基礎的な検討を行った。

2. 金属メッシュの諸特性とセンシング応用

(2・1) 金属メッシュの諸特性 金属メッシュは、図 1 に示すように金属の薄板に正方格子状の正方形開口を配列したもので、厚さ t 、金属ストリップの幅の半値 a 、開口の 1 辺と金属ストリップ幅を足し合わせた格子定数 g という 3 種類の機構的なパラメータで表すことができる。

金属メッシュの光学的な特性は、反射パワーを R 、透過パワーを T 、吸収を A 、回折を D とするとエネルギー保存の関係が成り立ち、 $R+T+A+D=1$ となり、一般的にハイパスフィルタ特性を有する。回折 D は、金属メッシュへの平面波の入射角を α とし、 $\lambda/g > 1 + \sin \alpha$ の波長域では現れず、この領域では透過率が高周波になるにつれて高くなってゆく。吸収 A はメッシュの金属部分が良導体である場合、表面電流による抵抗損で表すことができるが、この値は非常に小さな値となるため、無視することができ、 $R+T=1$ と近似できる⁽⁸⁾。回折が現れる波長域では、透過率が金属に対する開口の面積比よりも共鳴的に高くなる周波数領域が現れることが知られており、金属メッシュ表面において金属材料とその界面の誘電率および 2 次元周期構造により決まる表面プラズモンポラリトン (Surface Plasmon Polariton: SPP) ライクなモードによる表面波との結合と再放射に起因すると考えられている⁽¹⁰⁾。平坦な金属表面における SPP の分散関係は、金属の誘電率 ϵ_1 、金属に接する媒質の誘電率を ϵ_2 とすると、

$$k_x = \frac{\omega}{c} \sqrt{\frac{\epsilon_1 \epsilon_2}{\epsilon_1 + \epsilon_2}} \dots\dots\dots (1)$$

と表すことができる⁽¹¹⁾。ここで k_x は SPP の波数ベクトル、 c は真空中の光速である。但し、 $\epsilon_1 < 0$ 、 $\epsilon_2 \geq 1$ である。

金属 2 次元周期構造は、この表面波と結合する周波数が異常透過領域にあたり、 ϵ_2 を測定対象物とすると、測定対象物の密度や複素屈折率に応じて共鳴周波数が変化する。サブテラヘルツ領域では、波長程度の板厚を有する三角格子配列円形開口金属アレイを利用したセンシングが報告されている⁽¹²⁾。一方、金属メッシュはエレクトロフォーミング法による製造技術が確立されており、格子定数や開口幅をミクロン単位で設計することができ、あらゆるテラヘルツ帯の周波数に対応した設計が可能である。板厚は波長の数分の 1 から数十分の 1 と薄くなるため、近年技術の進歩がめざましい印刷技術を利用してさらに安価に作成することが期待できる。

テラヘルツ帯におけるセンシングの例としては、マイク

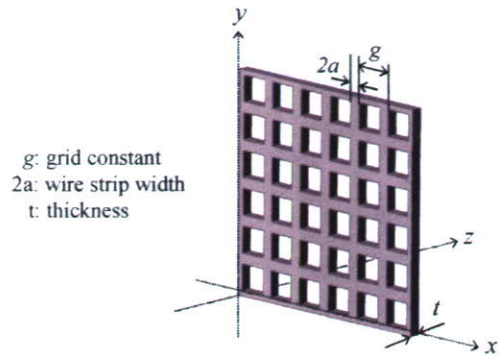


図 1 金属メッシュ
Fig. 1. A metallic mesh.

ロストリップライン共振器を用いた微量な DNA のラベルフリー検出の報告がある⁽¹³⁾。金属メッシュはセンシングエリアを 2 次元でとることができ、異なる多数のサンプルを金属メッシュに固定することにより、イメージングによる簡便かつ安価な生体高分子のラベルフリーセンシングや、高分子薄膜の品質検査などへの応用が期待できる。

(2・2) 電界分布および周波数特性の解析 金属メッシュのセンシング応用可能性を検討するにあたり、有限差分時間領域 (Finite Difference Time Domain: FDTD) 法を用いて金属メッシュ開口近傍の電磁界分布と、サンプル配置による周波数特性への影響を評価した。計算には Rsoft Design Group 社の FullWAVE⁽¹⁴⁾を使用した。図 1 の座標系に金属メッシュの開口を含む単位格子を配置し、平面波が $-z$ から $+z$ に向かって垂直入射するものとし、 $x-z$ 面と $y-z$ 面には周期境界条件を適用した。金属メッシュの機構的サイズは $g = 76.3 \mu\text{m}$ 、 $2a = 18.3 \mu\text{m}$ 、 $t = 6 \mu\text{m}$ とし、金属の誘電分散は、ニッケルのドルーデモデルを適用した⁽¹⁵⁾。電界分布を計算する周波数は、金属メッシュの機構的サイズから計算される透過率がピークとなる 3 THz とした⁽⁸⁾。

図 2 は金属メッシュの開口を含む単位格子 1 つ分の $x-z$ 面からみた電界強度分布であり、入射電界振幅に対して規格化した絶対値の分布を示した。図 2(a)は E_x 成分の電界強度分布である。紙面下方から平面波が金属メッシュに入射し、金属メッシュ開口内では局所的に電界が強くなり、裏面から数波長程度で再び平面波となって上方に伝搬していく様子がわかる。図 2(b)は、 E_z 成分の電界強度分布であり、図中の符号は電界の極性を表しており、金属メッシュ開口のエッジ部分で電界の極性が互い違いとなって局所的に強くなっていることがわかる。以上の結果から、これらの局所的に強い電界が現れる領域にサンプルに置いた場合、サンプルの密度や厚さによって (1) 式の ϵ_2 が変化し周波数特性が変化するものと考えられる。

次に、金属メッシュにサンプルを配置し、サンプル厚さの周波数特性への影響をシミュレーションにより見積もった。金属メッシュの金属部分にサンプルが均一にコーティングされた状態を想定し、サンプルの屈折率 $n = 1.5$ 、吸収係数 $\kappa = 0.01$ とし、サンプルの厚さ t が $2 \mu\text{m}$ と $4 \mu\text{m}$ の場

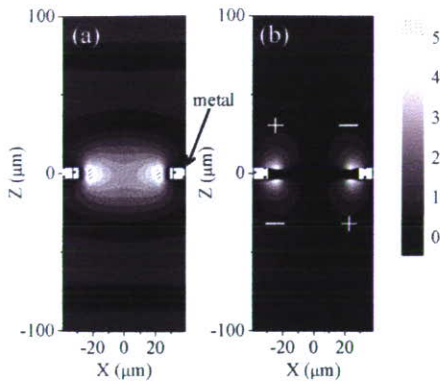


図2 金属メッシュ断面の電界分布：(a) E_x 成分，(b) E_z 成分
Fig. 2. Electric field distribution of cross section of metallic mesh for (a) Electric field of E_x and (b) E_z .

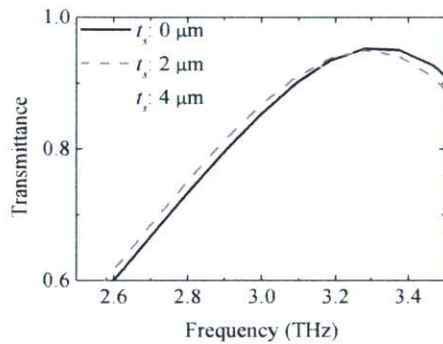


図3 シミュレーションによる金属メッシュにコーティングしたサンプル厚さと透過特性の依存性
Fig. 3. Calculated spectra of the metallic mesh and the dependence of the coated sample thickness.

合について計算を行った。図3は透過特性の計算結果である。サンプルの厚さに応じて透過特性が低周波側にシフトすること、吸収による透過率の減少が顕著に現れることを確認でき、金属メッシュがサンプルのわずかな厚さの変化に対して感度良く応答することがわかる。

3. 実験方法および結果

(3-1) 金属メッシュの透過特性 金属メッシュの機構的サイズと透過特性の関係を確認するため、格子定数 g が $50.8 \mu\text{m}$ から $254 \mu\text{m}$ まで6種類の金属メッシュを、エレクトロフォーミング法により作成した。材質はニッケルである。表1は作成した金属メッシュの機構的な仕様である。図4はこれらの金属メッシュをフーリエ変換式赤外分光光度計（日本分光製 FARIS-1S）によりメッシュ面に対して垂直にテラヘルツ波を入射して測定した透過特性である。いずれの金属メッシュも開口率が約60%であるが、透過率が0.8を上回っており異常透過現象が現れている。ピーク周波数は格子定数 g が小さくなるにつれ高周波側にシフトすることがわかる。また、ピーク周波数付近で透過率が急激に減少するディップがみられるが、これは測定に使用した

表1 金属メッシュの機構パラメータ

Table 1. Geometric parameters of the metallic meshes.

Mesh No.	Line / inch	g	2a	t
#1	500	50.8	17.8	6
#2	400	63.5	18.5	6
#3	333	76.3	18.3	6
#4	250	102	21.6	6
#5	150	169	34.0	22
#6	100	254	54.0	39

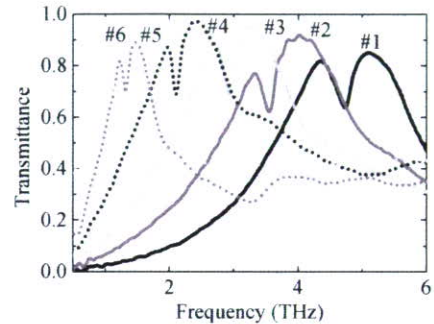


図4 6種類の金属メッシュの透過特性
Fig. 4. Measured transmission spectra of the 6 types of metallic meshes.

FTIRのビームが金属メッシュにて焦点を結ぶ集光系であることに起因し、Wood's anomalies であると考えられる。

(3-2) 微量生体高分子の定量的検出 金属メッシュに生体高分子を定量的に塗布し、透過特性を測定することによりセンシングの検証を行った。固定する生体高分子にはタンパク質の一種であるアビジン（ナカライテスク 純度97% 凍結乾燥粉末）を用い、滅菌蒸留水を溶媒とする溶液を作成した。アビジンは卵白中に存在する低塩基性糖タンパク質で、ビオチンと結合し、その親和力は強く不可逆であり、研究用試薬として広く利用されている。アビジンの定量的な塗布にはエレクトロスプレーデポジション（ElectroSpray Deposition: ESD）法⁽¹⁶⁾を用いた。図5はESD法によるタンパク質溶液の塗布を表した模式図である。タンパク質溶液は内径 $30 \sim 40 \mu\text{m}$ のガラス製のキャピラリーに収められ、そこに高圧電源に接続された電極が浸されている。対向するグラウンド面（金属メッシュ）と電極間に数千ボルトの電圧を印加すると、キャピラリー先端では電界が集中し、ある電圧に達すると表面張力との均衡が崩れ、サンプル溶液が飛び出し始める。飛び出した直後の液滴は強く帯電しているため、静電気力の反発により液滴が分裂し、粒径がナノサイズのパーティクルとなり、溶媒は瞬時に蒸発する。そしてナノサイズのパーティクルは静電気力によってグラウンド面に引き寄せられ堆積する。さらにこのプロセスは常温・常圧下で可能なため、タンパク質の失活を抑えることが可能である。テラヘルツ帯では水による吸収が非常に大きく水を含むサンプルの分析は一般的に困難であるが、本手法は分析に不要な水分を取り除くことができ、テ

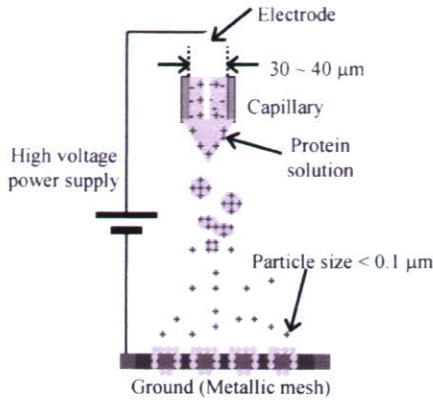


図5 ESD法を用いた金属メッシュへのタンパク質の塗布
Fig. 5. Schematic of spraying protein on to metallic mesh using the ESD method.

ラヘルツ帯におけるタンパク質のセンシングに適したサンプルの作成法になり得ると考える。

用意したサンプルを表2に示す。アビジンを塗布する基板は、表1の#3の金属メッシュ ($g: 76.3 \mu\text{m}$, $2a: 18.3 \mu\text{m}$, $t: 6 \mu\text{m}$) と、金属メッシュによるセンシングとの感度を比較するため、テラヘルツ帯で周波数特性がフラットな厚さ約 $10 \mu\text{m}$ のポリエチレン膜に白金をスパッタ (膜厚約 50 \AA) したものを用意した。ポリエチレン膜に白金をスパッタしたのは、ESD法を用いてタンパク質が基板に均一に塗布するためには基板が導電性を有している必要があるためである。これらの基板にESD装置 (Fuence社製 ES-1000) を用いてアビジン溶液を塗布した。アビジンを金属メッシュに塗布したサンプルを、電子顕微鏡を用いて観察した写真を図6に示す。10000倍にて観察したところ、メッシュの素材であるニッケル表面にアビジンを 200 ng/mm^2 塗布したものはアビジンが薄くコーティングされている様子が観察でき、 1200 ng/mm^2 になると、直径 $0.1 \mu\text{m}$ 以下のアビジンのパーティクルが堆積している様子がわかる。図7に作成したサンプルをそれぞれ前節と同様の方法で測定した 2.5 THz から 3.0 THz における透過特性を示す。上段(a)は、ポリエチレンに白金をスパッタした基板に 200 ng/mm^2 のアビジンを塗布したサンプルと、アビジンを塗布していない同一の基板のみの透過特性であり、アビジンの有無による明瞭な違いを確認することは出来ない。一方、下段(b)は、薄型金属メッシュにアビジンを塗布したサンプルの透過特性を示している。アビジンを塗布していない場合と比べ、アビジンの塗布量に応じて段階的に低周波側にシフトしている様子が確認でき、ディップの谷となる周波数はアビジンの無い場合の 2.82 THz から順に 2.81 THz , 2.64 THz とシフトしている。このことは、先のシミュレーション結果と合わせて考察すると、金属メッシュ開口近傍の局所的に電界の強い部分にアビジンを塗布することにより、アビジンの屈折率が濃度に応じて金属メッシュ上に局在する電界に影響を及ぼし、周波数特性の変化としてテラヘルツ帯で検出されていることを示している結果であると考えられる。

表2 ESD法により作成したサンプル

Table 2. Parameter of the ESD samples.

Sample No.	Substrate	Density of Avidin
#s1	Polyethylene membrane sputtered with platinum	200 ng/mm^2 (3.3 pmol)
#s2	Metallic mesh	200 ng/mm^2
#s3	Metallic mesh	1200 ng/mm^2 (19.8 pmol)

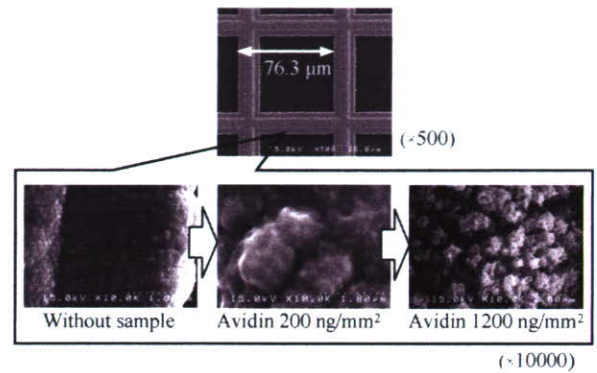


図6 アビジンを塗布した金属メッシュのSEM像
Fig. 6. SEM images of the metallic mesh with and without avidin.

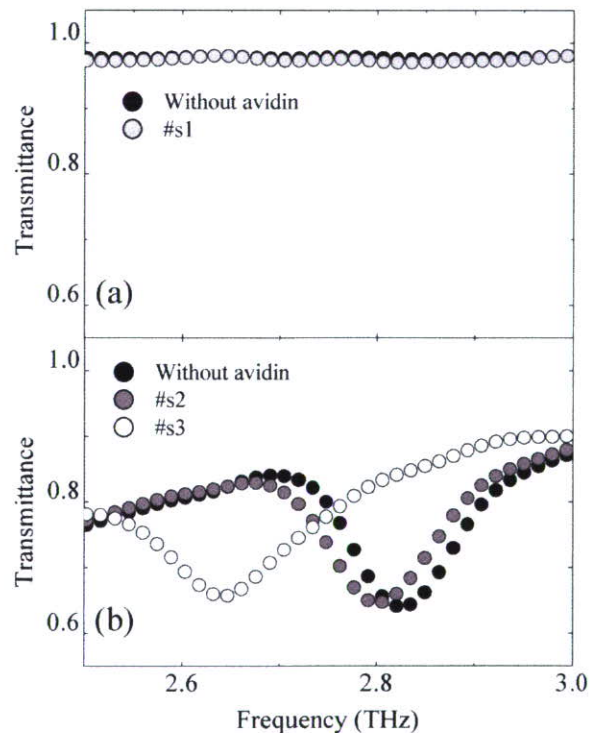


図7 作成したサンプルの透過特性: (a) #s1 と#s1の基板のみ, (b) #s2, #s3 と金属メッシュのみ
Fig. 7. Measured transmission spectra of the samples using the ESD method. (a) #s1 and the same substrate of #s1 without avidin. (b) #s2, #s3 and the same metallic mesh without avidin.

4. むすび

金属メッシュを用いたセンシング法の基礎検討を目的として、金属メッシュにテラヘルツ波を入射した場合の金属メッシュ近傍の電界分布計算から金属メッシュ開口内とエッジ部に局在する強い電界を確認し、サンプル配置による周波数特性変化の解析から、サンプルのわずかな厚さの変化に対して周波数特性が変化することを確認した。検証としてタンパク質の検出実験から、200 ng/mm² (3.3 pmol) という微量なタンパク質により透過特性が変化の様子を確認した。今後は更なる高感度化を目指し、メッシュ構造およびテラヘルツ波の入射条件について解析し、イメージングを取り入れたセンシングを行う予定である。

ESD法を用いたサンプル作成においてご協力いただきました株式会社フェーエンスの加瀬取締役副社長、最上主任研究員に深く感謝申し上げます。

(平成19年4月24日受付, 平成19年7月17日再受付)

文 献

- (1) K. Kawase, J. Shikata, and H. Ito : "Terahertz wave parametric source", *J. Phys. D: Appl. Phys.*, Vol.35, pp.R1-R14 (2002-1)
- (2) M. Hangyo, T. Nagashima, and S. Nashima : "Spectroscopy by pulsed terahertz radiation", *Meas. Sci. Technol.*, Vol.13, pp.1727-1738 (2002-10)
- (3) M. Brucherseifer, M. Nagel, P. Haring Bolivar, H. Kurz, A. Bosserhoff, and R. Büttner : "Label-free probing of the binding state of DNA by time-domain terahertz sensing", *Appl. Phys. Lett.*, Vol.77, Iss. 24, pp.4049-4051 (2000-11)
- (4) N. Karpowicz *et al.* : "Compact continuous-wave subterahertz system for inspection applications", *Appl. Phys. Lett.*, Vol.86, pp.054105 (2005-1)
- (5) K. F. Renk and L. Genzel : "Interference Filters and Fabry-Perot Interferometers for the Far Infrared", *Appl. Opt.*, Vol.1, No.5, pp.643-648 (1962-9)
- (6) K. Sakai, T. Fukui, Y. Tsunawaki, and H. Yoshinaga : "Metallic mesh bandpass filters and Fabry-Perot interferometer for the far infrared", *Jpn. J. Appl. Phys.*, Vol.8, No.8, pp.1046-1055 (1969-8)
- (7) R. Ulrich : "Far-Infrared Properties of Metallic Mesh and Its Complementary Structure", *Infrared Phys.*, Vol.7, Iss. 1, pp.37-55 (1967-1)
- (8) J. M. Lamarre, N. Coron, R. Courtin, G. Dambier, and M. Charra : "METALLIC MESH PROPERTIES AND DESIGN OF SUBMILLIMETER FILTERS", *Int. J. Infrared Millimeter Waves*, Vol.2, No.2, pp.273-292 (1981-3)
- (9) T. W. Ebbesen, H. J. Lezec, H. F. Ghaemi, T. Thio, and P. A. Wolff : "Extraordinary optical transmission through sub-wavelength hole arrays", *Nature*, Vol.391, pp.667 (1998-2)
- (10) H. F. Ghaemi, T. Thio, D. E. Grupp, T. W. Ebbesen, and H. J. Lezec : "Surface plasmons enhance optical transmission through subwavelength holes", *Phys. Rev. B*, Vol.58, Iss. 11, pp.6779-6782 (1998-9)
- (11) H. Raether : "Surface Plasmons on Smooth and Rough Surfaces and on Gratings", *Springer Tracts in Modern Physics* 111, p.5, Springer-Verlag, Berlin (1988)
- (12) F. Miyamaru, S. Hayashi, C. Otani, K. Kawase, Y. Ogawa, H. Yoshida, and E. Kato : "Terahertz surface-wave resonant sensor with a metal hole array", *Opt. Lett.*, Vol.31, Iss. 8, pp.1118-1120 (2006-4)
- (13) P. H. Bolivar, M. Brucherseifer, M. Nagel, H. Kurz, A. Bosserhoff, and R. Büttner : "Label-free probing of genes by time-domain terahertz sensing", *Phys. Med. Biol.*, Vol.47, No.21, pp.3815-3821 (2002-10)
- (14) http://www.rsoftdesign.com/products/component_design/FullWAVE/
- (15) M. A. Ordal, R. J. Bell, R. W. Alexander, Jr., L. L. Long, and M. R. Querry : "Optical properties of Au, Ni and Pb at submillimeter wavelengths", *Appl. Opt.*, Vol.26, Iss. 4, pp.744-752 (1987-2)
- (16) V. N. Morozov and T. Ya. Morozova : "Electrospray Deposition as a

Method To Fabricate Functionally Active Protein Films", *Anal. Chem.*, Vol.71, No.7, pp.1415-1420 (1999-4)

加藤 英志



(非会員) 1975年12月24日生。2000年3月名古屋工業大学大学院工学研究科博士前期課程修了。同年4月(株)アドバンテスト入社。2006年4月より名古屋大学大学院工学研究科博士後期課程在学中。現在、テラヘルツ波応用研究に従事。

吉田 永



(非会員) 1975年5月6日生。2001年3月東北大学大学院農学研究科博士前期課程修了。2004年10月より東北大学大学院農学研究科テラヘルツ生物学寄附講座技術補佐員。2006年10月より同大学大学院農学研究科博士後期課程在学中。現在、テラヘルツ波応用研究に従事

林 伸一郎



(非会員) 1974年5月12日生。2004年3月明治大学大学院理工学研究科博士後期課程修了(博士(理学))。2006年4月より同研究所緑川レーザー物理工学研究室協力研究員。2007年4月より東北大学大学院農学研究科助教を兼任。現在、テラヘルツ光源の研究に従事。

小川 雄一



(正員) 1971年5月16日生。1997年3月岡山大学大学院自然科学研究科修士課程修了。2005年7月同大学大学院農学研究科助教授(博士(農学))。2007年4月より同大学大学院農学研究科准教授。現在、テラヘルツ波の農業応用に関する研究に従事。

水津 光司



(非会員) 1974年1月24日生。2001年3月九州大学大学院工学研究科応用物理学専攻博士後期課程修了(博士(工学))。2007年4月より名古屋大学大学院工学研究科助教。現在、テラヘルツ光源・イメージングの研究に従事。

川瀬 晃道



(正員) 1966年9月14日生。1996年3月東北大学大学院工学研究科電子工学専攻博士課程修了(工学博士)。2007年4月より名古屋大学エコトピア科学研究所教授。現在、テラヘルツ光源・イメージングの研究に従事。

Terahertz sensing method for protein detection using a thin metallic mesh

H. Yoshida,^{a)} Y. Ogawa, and Y. Kawai

Graduate School of Agricultural Science, Tohoku University, 1-1 Tsutsumidori, Amemiya, Aoba, Sendai 981-8555, Japan

S. Hayashi

Laser Technology Laboratory, RIKEN, 2-1 Hirosawa, Wako 351-0198, Japan

A. Hayashi and C. Otani

Terahertz-wave Research Program, RIKEN, 519-1399 Aoba, Aramaki, Aoba, Sendai 980-0845, Japan

E. Kato

Advantest Laboratories, Ltd., 48-2 Matsubara, Kamiyashi, Aoba, Sendai 989-3124, Japan

F. Miyamaru

Faculty of Science, Shinshu University, 3-1-1 Asahi, Matsumoto, Nagano 390-8621, Japan

K. Kawase

EcoTopia Science Institute, Nagoya University, Furo-cho, Nagoya 464-8603, Japan

(Received 3 August 2007; accepted 27 November 2007; published online 18 December 2007)

A label-free biological sensor, which is based on the resonant transmission phenomenon of a thin metallic mesh, is proposed in the terahertz wave region. By using this sensor, we demonstrate the highly sensitive detection of small amounts of protein horseradish peroxidase. For quantitative investigation of the sensitivity of our sensor, horseradish peroxidase was printed on the metallic mesh surface by using a commercial available printer. A distinct shift of the transmission dip frequency is observed for 500 pg/mm² (11 fmol) of horseradish peroxidase printed on the metallic mesh, indicating the significantly high sensitivity of our sensor. © 2007 American Institute of Physics. [DOI: 10.1063/1.2825411]

In the past two decades, terahertz waves, located in the frequency region between the microwaves and the infrared, have found an increasing number of applications in various fields of research.¹⁻³ Especially, terahertz technology has a broad applicability in the biomedical context because the collective vibration modes of many protein and DNA molecules are predicted to occur in the terahertz range.^{4,5} The refractive index and absorption coefficients of single-stranded DNA and double-stranded DNA are different from each other in the terahertz region, indicating distinguishable characteristics.⁶ Reports have also been published on the avidin-biotin complex⁷ and the imaging of artificial RNA.⁸ These studies have revealed the potential applications of label-free sensings for many biomedical molecules by using the terahertz waves. In biomedicine, label substrates, which might involve fluorescence, an enzyme reaction, or a radioisotope are used for the detection of proteins. However, these procedures are complex and take a lot of time. The label-free detection with terahertz waves is a convenient technique in biomedicine, which enables us to realize easier and faster medical and food inspections than other techniques.

In this paper, we propose a label-free sensing method using a thin metallic mesh in the terahertz region. The transmission characteristics of thin metallic meshes, investigated since the 1960s,^{9,10} are those of a band-pass filter in the far-infrared region. This is due to the resonant transmission caused by an excitation of surface plasmon polaritons¹¹ (SPPs). The transmission properties of a thin metallic mesh are determined mainly by its geometric parameters, but, when a material is placed near the mesh openings, are also

affected by the refractive index of that material, in the sense that a shift of the resonant transmission frequency occurs.^{12,13} Our sensing method is based on the change of the transmittance of terahertz radiation through a thin metallic mesh accompanied by the resonant frequency shift when a sample substance is applied on the mesh openings. The transmittance of the thin metallic mesh does not change due to the absorption, but dominantly due to the variation of the refractive index of the sample substances near the openings.¹⁴ Using this thin metallic mesh sensor, we detected the protein horseradish peroxidase, which is an oxidation/reduction enzyme existing in many organisms and is typically used as an indicator in biochemical reactions. The horseradish peroxidase is one of the most widespread label substrates in biomedicine.

In our experiment, the thin metallic mesh was made from electroformed nickel, allowing the fabrication of a smooth surface and precise periodicity of the grating. The two dimensional square metallic mesh was 6 μm thick with a grating period of 76.3 μm and a metallic linewidth of 18.3 μm, in both dimensions. This metallic mesh behaves as a high-pass filter and the peak transmission is approximately 95% at 3.37 THz. We measured the transmission spectra of a thin metallic mesh using a Fourier transform infrared spectrometer (FARIS-1S; JASCO, Japan), in which the terahertz beam was focused into an area of about 7 mm in diameter on the thin metallic mesh (Fig. 1). We used the protein horseradish peroxidase (Nacalai Tesque) as a sample, by dissolving it in sterilized pure water at the concentrations of 1.0, 0.5, 0.25, and 0.125 mg/ml. These enzyme solutions were spread on the thin metallic mesh. For a quantitative investigation of the sensitivity of the metallic mesh sensor, the accurate spreading of sample substances on the sensor is criti-

^{a)}Electronic mail: yoshida_h@bios.tohoku.ac.jp. Tel./FAX: +81-22-717-8946.

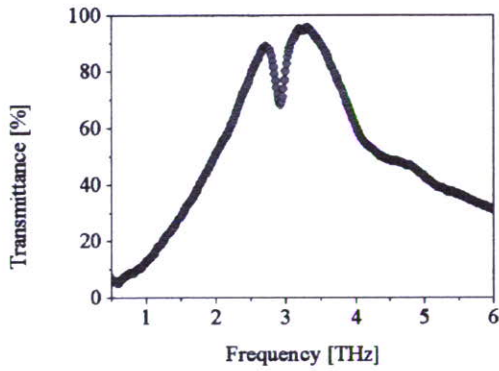


FIG. 1. Measured transmission spectrum of a thin metallic mesh with a grating period of 76.3 μm and a metallic linewidth of 18.3 μm .

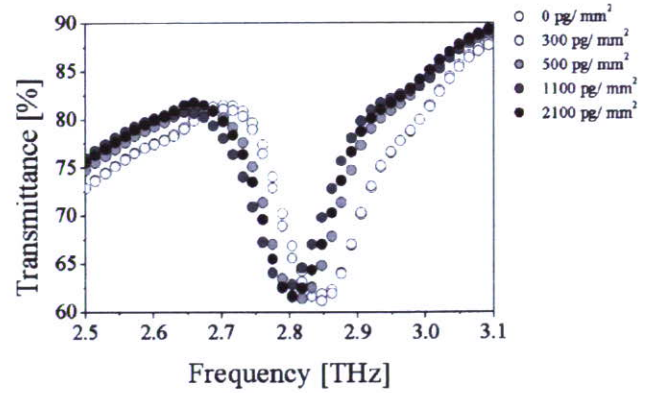
cally important. We printed horseradish peroxidase on the metallic meshes using a commercial inkjet printer (Pixus 860i; Canon, Tokyo, Japan), the same that was previously used to fix DNA on a chip.¹⁵ The amount of the sample was controlled using an image processing software. By using the inkjet printer, a considerably small amount of sample can be spread on various materials more readily than with other printing systems.

Figure 1 shows the transmission spectrum of the thin metallic mesh. The broad transmission peak is observed at 3.37 THz and the peak transmittance exceeds the fraction of a mesh opening. This resonant transmission phenomenon is derived from the resonant excitation of SPPs. The resonant frequency of the SPP is expressed as

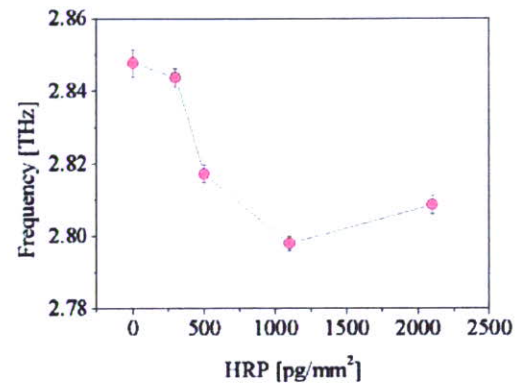
$$f_{\text{SPP}} = |\mathbf{k}_{\text{in}} + \mathbf{G}| \frac{c}{2\pi} \left(\frac{\epsilon_m + \epsilon_d}{\epsilon_m \epsilon_d} \right)^{1/2}, \quad (1)$$

where \mathbf{k}_{in} is the in-plane wave-vector of the incident terahertz wave, \mathbf{G} is the reciprocal lattice vector of the periodic structure, and ϵ_m and ϵ_d are the dielectric constants of the metal and the interface medium. The discrepancy between the observed peak frequency (3.37 THz) and the resonant frequency of SPPs (3.93 THz) expected from the Eq. (1) is attributed to the Fano-like interference effect between the terahertz waves transmitted directly through metal openings and reemitted from the SPPs excited on the metal surface.^{16,17} In Fano's original study, he investigated the situation of the interference between two contributions, a non-resonant continuum state and a resonant discrete one. For the problem of transmission of terahertz wave through metal mesh, the former corresponds to the directly transmitted terahertz wave and later corresponds to the reemitted terahertz wave from SPPs. This Fano-like interference leads to the asymmetric spectral shape around the resonant frequency and, consequently, the redshift of the transmission peak with respect to the SPP resonant frequency.

When we used collimated incident terahertz waves, this transmission dip is not observed at normal incidence while it is observed at oblique incidences (not shown). In addition, the transmission dip frequency shows the incident angle dependence. From these results, the observed transmission dip arises as a result of the transmission peak splitting for oblique incidence. For the square lattice structured surface, the first order SPP mode splits into two modes analogous to photonic band modes in photonic crystals.^{18,19} In this case, the spectral dip is possibly observed between transmission



(a)



(b)

FIG. 2. (Color online) (a) Measured transmission spectra of a thin metallic mesh with various concentrations of horseradish peroxidase. (b) The transmission dip frequency as a function of the horseradish peroxidase concentration.

peaks of these two modes. For the focused incident beam, like our experiment, the component of oblique incident terahertz wave involved and, thus, the transmission dip appears as the integral of the contributions from several oblique components. Since the resonant frequencies of the transmission peak and dip strongly depend on the refractive index in the vicinity of the metallic mesh openings, the extremely small amount of the sample substances can be detected by monitoring the position of the transmission peak and/or dip.

Figure 2(a) shows the measured transmission spectra of the thin metallic mesh with various amounts of peroxidase printed on it. We present the transmission spectra only in the frequency range around the transmission dip observed in Fig. 2. The transmission dip frequency shows a tendency to decrease with increasing the amount of sprayed peroxidase. The transmission dip frequency, which is estimated from the fitting of the measured spectrum with a Lorentz function, is plotted in Fig. 2(b) as a function of the amount of peroxidase. A clear frequency shift of the transmission dip is observed for 500–2100 pg/mm^2 horseradish peroxidase with respect to that of the bare metallic mesh (0 pg/mm^2). This result indicates that the sensing with thin metallic meshes is extremely sensitive for the detection of very small amounts of biomolecules, equal to the sensitivity of the conventional method using an antibody labeled horseradish peroxidase.

Nagle *et al.* reported the detection of the femtomole order of

DNA by using a coplanar waveguide with a resonant structure²⁰ and at functionalized electrodes via hybridization in the terahertz region.²¹ Our thin metallic mesh sensing can detect proteins in the order of femtomole, which should allow the application of our sensor to protein detection in biomedicine.

The peak frequency basically shifts to the lower frequency side with increasing the volume of the horseradish peroxidase in the range from 300 to 2100 pg/mm². The peak frequency for 2100 pg/mm², however, returns slightly to the higher frequency with respect to that for 1100 pg/mm². This result is due to the inhomogeneous spreading of the horseradish peroxides on the metallic mesh in our printing system. More precise spreading can help to avoid this ambiguity in the detection of the frequency shift.

The transmittance at the dip frequency changes only slightly with the volume of the horseradish peroxides. This indicates that the absorption of the terahertz wave by the sample substances plays a minor role for the variation of the transmission spectrum. Such a small variation of the transmittance makes it difficult to detect the sample substances by monitoring the transmission intensity at a single frequency.

In conclusion, we demonstrated the highly sensitive detection of protein molecules in amounts in the femtomole order by using a thin metallic mesh sensor. For spreading the extremely small amount of sample substances on the metallic mesh sensor, we used a commercially available printer with which horseradish peroxidase could be printed. For the metallic mesh sensor printed with 500 pg/mm² (11 fmol) horseradish peroxidase, a redshift of the transmission dip frequency is observed clearly, which is based on the variation of the refractive index in the vicinity of the metallic mesh openings. This result exceeds the detection limit of conventional terahertz spectroscopy for protein molecules. As a next challenge, we aim to achieve a label-free selective detection of proteins by using an antigen/antibody reaction.

This work was supported in part by a Grant-in-Aid for Young Scientists (18070501) from The Ministry of Health, Labour and Welfare of Japan.

- ¹M. Tonouchi, *Nat. Photonics* **1**, 97 (2007).
- ²B. Ferguson and X.-C. Zhang, *Nat. Mater.* **1**, 26 (2002).
- ³A. Dobroui, R. Beigang, C. Otani, and K. Kawase, *Appl. Phys. Lett.* **86**, 261107 (2005).
- ⁴A. Markelz, S. Whitmire, J. Hillebrecht, and R. Birge, *Phys. Med. Biol.* **49**, 3798 (2002).
- ⁵B. M. Ficher, M. Walther, and P. U. Jepsen, *Phys. Med. Biol.* **47**, 3807 (2002).
- ⁶M. Nagle, P. Haring Bolivar, M. Brucherseifer, and H. Kruz, *Appl. Phys. Lett.* **80**, 154 (2002).
- ⁷S. P. Mickan, A. Menikh, H. Liu, C. A. Mannella, R. MacColl, D. Abbott, A. Munch, and X.-C. Zhang, *Phys. Med. Biol.* **47**, 3789 (2002).
- ⁸B. M. Fischer, M. Hoffman, H. Helm, R. Wilk, F. Rutz, T. Klein-Ostmann, M. Koch, and P. U. Jepsen, *Opt. Express* **13**, 5205 (2005).
- ⁹R. Ulrich, *Infrared Phys.* **7**, 37 (1967).
- ¹⁰K. Sakai, T. Fukui, Y. Tsunawaki, and H. Yoshinaga, *Jpn. J. Appl. Phys., Part 1* **8**, 1046 (1969).
- ¹¹H. Raether, *Surface Plasmons on Smooth and Rough Surfaces and on Gratings* (Springer, Berlin, 1988).
- ¹²F. Miyamaru and M. Hangyo, *Appl. Phys. Lett.* **84**, 2742 (2004).
- ¹³H. Cao and A. Nahata, *Opt. Express* **12**, 1004 (2004).
- ¹⁴F. Miyamaru, S. Hayashi, C. Otani, K. Kawase, Y. Ogawa, H. Yoshida, and E. Kato, *Opt. Lett.* **31**, 1118 (2006).
- ¹⁵T. Okamoto, T. Suzuki, and N. Yamamoto, *Nat. Biotechnol.* **18**, 438 (2000).
- ¹⁶L. Martin-Moreno, F. J. Garcia-Vidal, H. J. Lezec, K. M. Pellerin, T. Thio, J. B. Pendry, and T. W. Ebbesen, *Phys. Rev. Lett.* **86**, 1114 (2001).
- ¹⁷E. Popov, M. Nevriere, S. Enoch, and R. Reinisch, *Phys. Rev. B* **62**, 16100 (2000).
- ¹⁸J. D. Joannopoulos, R. D. Meade, and J. N. Winn, *Photonic Crystal* (Princeton University Press, Princeton, 1995).
- ¹⁹H. F. Ghaemi, T. Thio, D. E. Grupp, T. W. Ebbesen, and H. J. Lezec, *Phys. Rev. B* **58**, 6779 (1998).
- ²⁰M. Nagle, P. H. Bolivar, M. Brucherseifer, and H. Kruz, *Appl. Phys. Lett.* **80**, 154 (2002).
- ²¹M. Nagle, F. Richter, P. H. Bolivar, and H. Kruz, *Phys. Med. Biol.* **48**, 3625 (2003).

THz sensing method based on metallic mesh and application to high-resolution sensing and imaging

E. Kato, S. Yoshida, H. Yoshida, A. Hayashi, S. Hayashi, Y. Ogawa, C. Otani and K. Kawase

Abstract— We report on a sensing method in the terahertz range using metallic mesh (MM). Conventionally, the filter property of an MM can be changed by the geometrical parameters of the MM. Considering that this property is also changed when the medium in the vicinity of the mesh openings has a different permittivity, we were able to measure small amounts of absorbing materials and thin plastic films on the metallic mesh. We observed change of both the transmission characteristics and the images.

Index Terms—imaging, metallic mesh, sensing, surface wave

I. INTRODUCTION

Metallic meshes (MMs), metallic membranes with a two-dimensional array of sub-wavelength holes, have been used as quasi-optical components such as mirrors, beam splitters, filters, and Fabry-Perot interference filters in the spectral region from microwave to far infrared [1]. The transmission characteristics of MMs can be determined by the shape and the arrangement of the apertures [2], [3]. The phenomenon of resonance enhanced transmission peaks observed for MMs is attributed not only to the waveguide mode but also to the resonant excitation of surface waves at the metal-air (or dielectric) boundaries of MMs [4]. Since the resonant frequency and transmittance are strongly affected by changes in the dielectric constant of the medium near the mesh openings, we can infer that small amounts of samples, attached on the metal surface, can be detected with high sensitivity [5].

E. Kato is with the Advantest Labs. Ltd., Sendai 989-3124 Japan (e-mail: eiji.kato@jp.advantest.com).

H. Yoshida and Y. Ogawa are with the Graduate School of Agricultural Science, Tohoku University, Sendai 981-8555, Japan (email: yoshida_h@bios.tohoku.ac.jp; yogawa@bios.tohoku.ac.jp).

A. Hayashi, S. Hayashi and C. Otani are with Terahertz-wave Research Program, RIKEN, Sendai 980-0845, Japan (email: ahayashi@riken.jp; shayashi@riken.jp; otani@riken.jp).

S. Yoshida and K. Kawase are with the EcoTopia Science Institute, Nagoya University, Nagoya 464-8603, Japan (email: h076433m@mbox.nagoya-u.ac.jp; kawase@nuee.nagoya-u.ac.jp).

II. EXPERIMENTS

A. Transmission properties of MM

We measured the basic transmission property of bare MM. Fig. 1 shows the transmission spectrum of the bare MM produced by the electroforming method with a focused beam under normal incidence using a standard THz-TDS system. The schematic of the MM is shown in the inset of Fig. 1. The grid constant of the MM is $g = 254 \mu\text{m}$, wire strip width $2a = 74 \mu\text{m}$ and thickness $t = 60 \mu\text{m}$. The enhanced transmission peak is observed at frequencies around 1 THz. The maximum transmittance at 1.03 THz is two times higher than that expected from the porosity of the mesh holes, and there exists one sharp dip at 0.99 THz. This sharp dip is attributed to anomalous diffraction when the THz wave incidents to the MM obliquely, similar to Wood's anomaly [6].

B. THz sensing of small amount of samples using MM

To investigate the quantitative responsiveness of the MM as a sensor, we used a commercial ink-jet printer (Pixus BJ F900, Canon, Tokyo, Japan) for quantitative ink sample ($n \sim 2.1$, $\kappa \sim 0.2$) spread. The amount of ink sample was controlled using image processing software. We prepared two types of substrates for comparison: the MM and a 0.1 mm thick PET film. The printed ink density on the PET film substrates was 40, 45 and 50 ng/mm^2 , respectively. Given that the porosity of the MM holes is about 50%, the estimated density of the ink printed on the MM is one-half that of the PET film substrate. For this

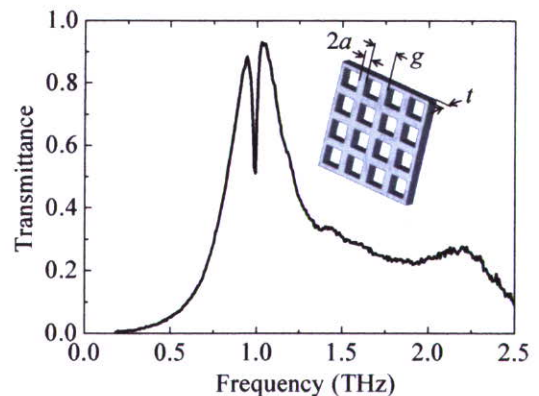


Fig. 1 Transmission spectrum of the metallic mesh used in the experiment.

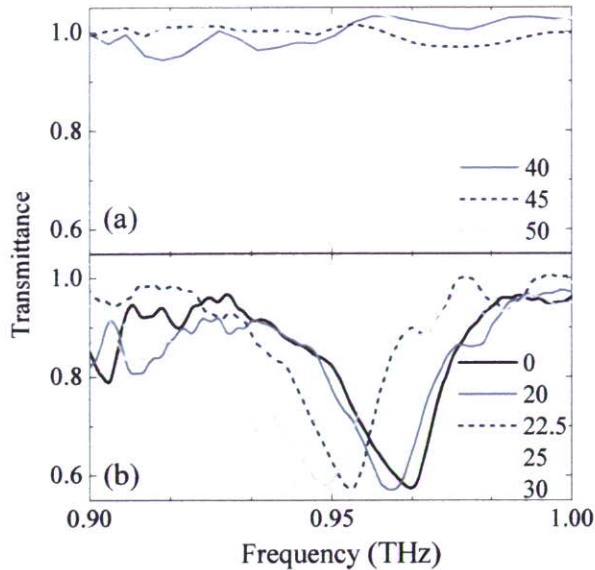


Fig. 2 Transmission spectra of printed ink samples. (a) without MM, (b) with MM. Unit of ink density is ng/mm^2 .

experiment, we set up a spectroscopic and imaging system using a backward wave oscillator (BWO) as a THz wave source (0.85 ~ 1.10 THz) and a deuterated L-alanine triglycine sulphate (DLATGS) detector [7]. THz waves radiating from the BWO are collimated by an off-axis parabolic mirror and focused onto the sample by another mirror. For image acquisition, the sample is x-y scanned using a linear motor stage that moves it through the focused beam. Fig. 2(a) shows the transmission spectra of the PET film substrate with the aforementioned densities of ink. There is no significant change even at higher ink densities. Fig. 2(b) shows the transmission spectra of the MM substrates with some ink densities and without ink. The lower shift of dip frequencies with increasing ink density is clearly observed relative to the bare MM, and a difference of $2.5 \text{ ng}/\text{mm}^2$ ink density could be detected; such a difference is difficult to detect using conventional THz spectroscopy. These shifts are believed to be caused by changes in the dielectric constant in the vicinity of the MM surface when small amounts of ink are printed on the MM.

C. THz imaging of thin materials using MM

For highly sensitive sensing by imaging, we used thin free-standing Teflon foils (Nilaco Co., Tokyo, Japan) of 5, 12, 20 and $25 \mu\text{m}$ thickness as samples. We attached the samples on both 0.1 mm thick paper and the MM, and imaged them using the aforementioned experimental setup. Fig. 3(b) of the THz transmission image of the samples attached on the MM at 0.96 THz shows that the thickness of the samples could be determined based on the transmitted power, and a difference of $5 \mu\text{m}$ thickness could be distinguished. However, such a difference could not be determined for the paper since there is no detectable contrast even for increased sample thickness (Fig. 3(a)).

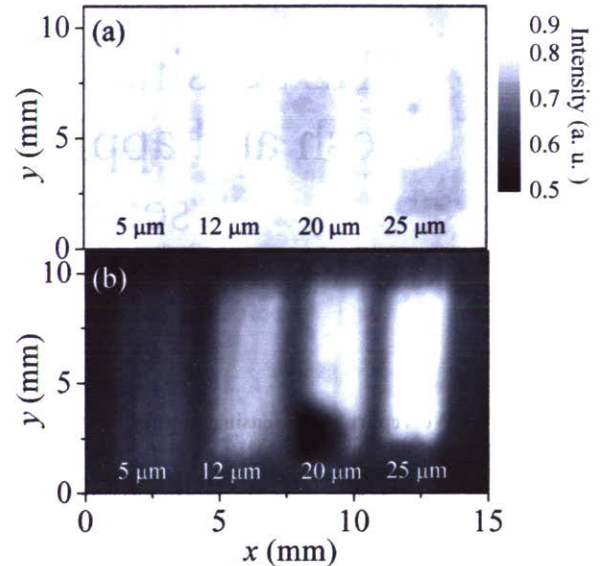


Fig. 3 Transmission image of the thin Teflon films. (a) without MM. (b) with MM.

III. CONCLUSION

We demonstrated highly sensitive sensing using MM, based on changes in the transmission characteristics produced by a variation of the dielectric constant near the mesh openings. Small amounts of absorbing substances printed on the MM can thus be detected, and a film sample much thinner than the THz wave can also be distinguished by imaging. This result suggests the possibility of label-free sensing of biological affinities, such as in the case of DNA hybridization or protein interactions, and a method for producing a simple, inexpensive sensor chip using a printing technology. We plan to investigate the MM sensor mechanism in further detail and will attempt to enhance its present sensitivity.

REFERENCES

- [1] K. Sakai, T. Fukui, Y. Tsunawaki and H. Yoshinaga, "Metallic mesh bandpass filters and Fabry-Perot interferometer for the far infrared," *Jpn. J. Appl. Phys.*, vol. 8, no. 8, pp.1046-1055, Aug. 1969
- [2] R. Ulrich, "Far-infrared properties of metallic mesh and its complementary structure," *Infrared Phys.*, vol. 7, iss. 1, pp.37-55, Jan. 1967.
- [3] K. Sakai and L. Genzel, "Far-infrared metal mesh filter and Fabry-Perot interferometry," in *Reviews of Infrared and Millimeter Waves*, vol. 1, K. J. Button, Ed. New York: Plenum, 1983, pp. 155-247
- [4] H. F. Ghaemi, T. Thio, D. E. Grupp, T. W. Ebbesen and H. J. Lezec, "Surface plasmons enhance optical transmission through subwavelength holes," *Phys. Rev. B*, vol. 58, iss. 11, pp. 6779-6782, Sep. 1998.
- [5] F. Miyamaru, S. Hayashi, C. Otani, K. Kawase, Y. Ogawa, H. Yoshida and E. Kato, "Terahertz surface-wave resonant sensor with a metal hole array," *Opt. Lett.*, vol. 31, iss. 8, pp. 1118-1120, Apr. 2006.
- [6] J. M. Lamarre, N. Coron, R. Courtin, G. Dambier and M. Charra, "METALLIC MESH PROPERTIES AND DESIGN OF SUBMILLIMETER FILTERS," *Int. J. Infrared Millimeter Waves*, vol. 2, no. 2, pp. 273-292 Mar. 1981.
- [7] A. Dobroiu, C. Otani and K. Kawase, "Terahertz-wave sources and imaging applications," *Meas. Sci. Technol.*, vol. 17, no. 11, pp.R161-R174, Nov. 2006.

Label-free Immunoassay by the Resonant Transmission Phenomenon of a Thin Metallic Mesh

Hisa Yoshida¹, Yasuhide Kawai¹, Shin'ichiro Hayashi², Eiji Kato³, Masato Oikawa⁴, Teruo Miyazawa¹, Chiko Otani⁵, Kodo Kawase⁶ and Yuichi Ogawa¹

1. Graduate School of Agricultural Science, Tohoku University, Sendai, Japan

2. Laser Technology Laboratory, RIKEN, Wako, Japan

3. ADVANTEST Laboratories, Ltd. Sendai, Japan

4. Graduate School of Life Sciences, Tohoku University, Sendai, Japan

5. Terahertz-wave Research Program, RIKEN, Sendai, Japan

6. EcoTopia Science Institute, Nagoya University, Nagoya, Japan

Abstract:

We propose a new label-free sensor of protein using a metallic mesh in Terahertz (THz) region. Our sensing method relies on a change in the transmittance of THz radiation passed through the metallic mesh on which a sample substance is contacted. Label-free detection using THz radiation is a new technique in biomedicine, which enable us to take easier and faster medical and food inspections.

By using this technique, we demonstrated the highly sensitive detection the protein horseradish peroxidase, which is an oxidation/reduction enzyme that exists in many organisms. For quantitative investigation of the sensitivity of our sensor, the enzyme was printed on surface of the metallic mesh by a commercial printer. A distinct shift in the transmittance spectrum toward lower frequency was observed for 500 pg/mm² (11 fmol) enzyme printed on the metallic mesh. Next we demonstrated to detect a streptavidin-biotin interaction on a PVDF membrane which is generally used fixation of protein and DNA. The streptavidin-biotin interaction can be detected by using 650 pg/mm² (2.5 pmol) biotin. These results indicate that our sensing system has high sensitivity and we have successfully demonstrated a convenient sensing system by using a metallic mesh and a PVDF membrane.

Keywords: label-free immunoassay, metallic mesh, Terahertz radiation, membrane

1. INTRODUCTION

Immunoassay is one of the most popular methods in biomedicine, which is based on antigen/antibody reaction using specific antibody. This method generally needs label materials, which might involve fluorescence, an enzyme reaction, or radioisotope, for highly sensitive detection. However the procedure is complex and takes a lot of time. On the other hand, Terahertz (THz) technology has broad applicability in a biomedical context and facilitates various applications because the collective vibration modes of many protein and DNA molecules are predicted to occur in the THz range.

In this paper, we propose a label-free sensing method using a thin metallic mesh in the THz region. The transmission characteristics of thin metallic meshes, investigated since the 1960s [1,2], are those of a band-pass filter in the far-infrared region. This is due to the resonant transmission caused by an excitation of surface plasmon polaritons (SPPs) [3]. The transmission properties of a thin metallic mesh are determined mainly by its geometric parameters, but, when a material is placed near the mesh openings, are also affected by the refractive index of that material, in the sense that a shift of the resonant transmission frequency occurs. [4,5] Our sensing method is based on the change of the transmittance of THz radiation through a thin metallic mesh accompanied by the resonant frequency shift when a sample substance is applied on the mesh openings. The transmittance of the thin metallic mesh does not change due to the absorption, but

dominantly due to the variation of the refractive index of the sample substances near the openings [6]. Using this thin metallic mesh sensor, we detected the protein horseradish peroxidase, which is an oxidation/reduction enzyme existing in many organisms and is typically used as an indicator in biochemical reactions. Horseradish peroxidase is one of the most widespread label substrates in biomedicine. Next by using PVDF membrane and a thin metallic mesh, we have demonstrated to detect streptavidin (240 kDa)-biotin complex.

2. EXPERIMENT

2.1 Properties of a thin metallic mesh

In our experiment, the thin metallic mesh was made from electroformed nickel, allowing the fabrication of a smooth surface and precise periodicity of the grating. The two dimensional square metallic mesh was 6 μm thick with a grating period of 76.3 μm and a metallic line width of 18.3 μm, in both dimensions. This metallic mesh behaves as a high-pass filter and the peak transmission is approximately 95 % at 2.8 THz. We measured the transmission spectra of a thin metallic mesh using a Fourier Transform Infrared (FT-IR) spectrometer (FARIS-1S; JASCO, Japan), in which the THz beam was focused into an area of about 5 mm in diameter on the thin metallic mesh.

Figure 1 shows the transmission spectrum of thin metallic mesh as a function of the wavelength λ normalized by the grating period g . The transmittance at the peak

wavelength observed at $\lambda / g = 1.23$, which is slightly longer than $\lambda / g = 1$, is 1.65 times as high as the opening fraction of the metallic mesh (57.8 %). This resonant transmission phenomenon is based on the interference effect between the THz waves transmitted directly through metal openings and reemitted from the surface plasmon polaritons excited on the metal surface [7,8]. In addition, a sharp transmission dip is observed at wavelength of $\lambda / g = 1.5$. This transmission dip appears as the result of the splitting of the surface plasmon polariton modes for the oblique incidence [9] derived by the focused THz radiation beam in our experimental setup. Since the resonant frequencies of the transmission peak and dip strongly depend on the refractive index in the vicinity of the metallic mesh openings, the extremely small amount of the sample substances can be detected by monitoring the position of the transmission peak and/or dip.

2.2 Highly sensitive detection of a protein horseradish peroxidase

We used the protein horseradish peroxidase (Nacalai Tesque) as a sample, by dissolving it in sterilized pure water at the concentrations of 1.0, 0.5, 0.25, and 0.125 mg/ml. These enzyme solutions were spread on the thin metallic mesh. For a quantitative investigation of the sensitivity of the metallic mesh sensor, the accurate spreading of sample substances on the sensor is critically important. We printed horseradish peroxidase on the metallic meshes using a commercial inkjet printer (Pixus 860i; Canon, Tokyo, Japan), the same that was previously used to fix DNA on a chip [10]. The amount of the sample was controlled using an image processing software. By using the inkjet printer, a considerably small amount of sample can be spread on various materials more readily than with other printing systems.

Figure 2(a) shows the measured transmission spectra of the thin metallic mesh with various amounts of peroxidase printed on it. We present the transmission spectra only in the wavelength range around the transmission dip observed in Fig. 2. The transmission dip frequency shows a tendency to decrease with increasing the amount of sprayed peroxidase. The transmission dip frequency, which is estimated from the fitting of the measured spectrum with a Lorentz function, is plotted in Fig. 2(b) as a function of the amount of peroxidase. A clear frequency shift of the transmission dip is observed for 500 – 2100 pg/mm^2 horseradish peroxidase with respect to that of the bare metallic mesh (0 pg/mm^2). This result indicates that the sensing with thin metallic meshes is extremely sensitive for the detection of very small amounts of biomolecules, equal to the sensitivity of the conventional method using an antibody labeled horseradish peroxidase. The peak frequency basically shifts to the lower frequency side with increasing the volume of the horseradish peroxidase in the range from 300 to 2100 pg/mm^2 . The peak frequency for 2100 pg/mm^2 , however, returns slightly to the higher frequency with respect to that for 1100 pg/mm^2 . This result is due to the inhomogeneous spreading of the horseradish peroxides on the metallic mesh in our printing system. More precise spreading can help to avoid this ambiguity in the detection of the frequency shift.

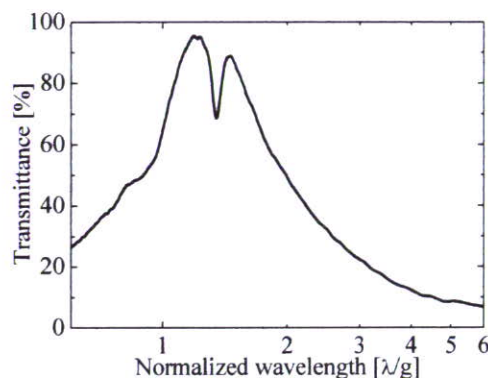


Fig.1. Measured transmission spectrum of a thin metallic mesh with grating period of 76.3 μm and a metallic line width of 18.3 μm .

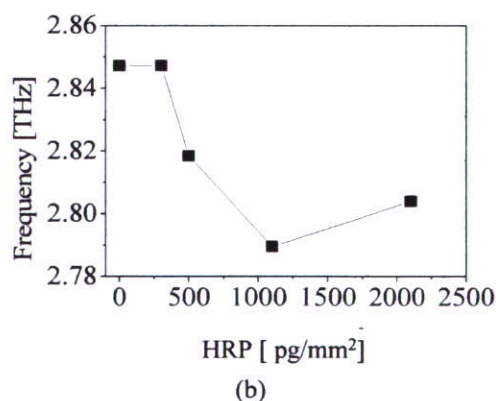
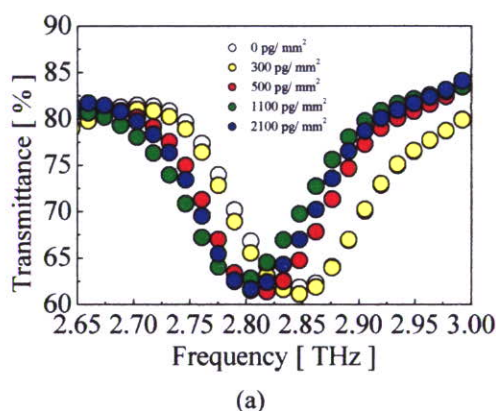


Fig. 2. (a) Measured transmission spectra of a thin metallic mesh with various concentrations of horseradish peroxidase. (b) The transmission dip frequency as a function of the horseradish peroxidase.

The transmittance at the dip frequency changes only slightly with the volume of the horseradish peroxides. This indicates that the absorption of the THz wave by the sample substances plays a minor role for the variation of the transmission spectrum. Such a small variation of the transmittance makes it difficult to detect the sample sub-

stances by monitoring the transmission intensity at a single frequency. However, owing to the shift of the resonant frequency depending on the refractive index in the vicinity of the metallic openings, a sensitive detection of the sample substances becomes possible with the single frequency source in the THz regime. In our experiments, a variation of more than 18 % in the transmission is observed at 2.9 THz for 1100 pg/mm² with respect to the bare metallic mesh. If we assume that the uncertainty of the transmittance in our experimental setup is less than 1 %, it follows that we can detect the horseradish peroxidase of at least 60 pg/mm² (a few fmol), which is never detected by conventional THz spectroscopy.

2.3 Detection of streptavidin-biotin interaction on PVDF membrane

Streptavidin (240 kDa) is a protein which binds biotin. Streptavidin-biotin complex has a low dissociation constant of about 10⁻¹⁵ M. Bovine serum albumin (BSA) (Albumin bovine serum, powder ;SIGMA) was labeled biotin (EZ-Link Sulfo-NHS-Biotinylation Kit: Pierce Biotechnology, Inc.) and applied on PVDF membrane (Immun-Blot™ PVDF Membrane; Bio-Rad) which generally used for fixation protein and DNA. These membrane which put in biotinylated-BSA, were into 0.1 % BSA solution (0.1 % BSA 20mM Tris, 500 mM NaCl, 0.05 % Tween-20, pH 7.5) for a prevention that other protein were attached these membrane. Streptavidin-biotin interaction was occurred in TTBS buffer (20 mM Tris, 500 mM NaCl, 0.05 % Tween-20, pH 7.5), after the process these membrane were washed TTBS buffer and pure water.

A thin metallic mesh (6 μm thick with a grating period of 76.3 μm and a metallic line width of 18.3 μm,) was fixed a circular holder and adhered with these membrane using a suction pump. We measured the transmission spectra of a thin metallic mesh with membrane using a Fourier Transform Infrared (FT-IR) spectrometer.

The transmission dip frequency, which is estimated from the fitting of the measured spectrum with a Lorentz function, is plotted in Fig. 3 as streptavidin-biotin interaction. When PVDF membrane was set on the metallic mesh, the peak frequency shift to the lower frequency side. This phenomenon based on a refractive index of PVDF membrane. In a case of biotinylated-BSA were applied on PVDF membrane, the peak frequency further

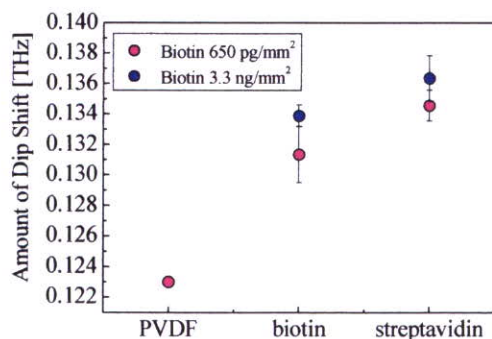


Fig. 3. The transmission dip frequency as streptavidin-biotin interaction.

shift to the lower frequency side. Finally streptavidin bind to biotinylated-BSA, amount of a dip shift was largest in the reaction. The refractive index of streptavidin-biotin complex was larger than biotinylated-BSA. Amount of dip shift increased on a concentration of biotin. The measurement of a transmittance without the metallic mesh could not detect streptavidin-biotin interaction. In our label-free sensing using the metallic mesh, 650 pg/mm² (2.5 pmol) biotin could be detected by the shift.

3. CONCLUSION

In conclusion, we demonstrated the highly sensitive detection of protein molecules in amounts in the fmol order by using a thin metallic mesh sensor. For spreading the extremely small amount of sample substances on the metallic mesh sensor, we used a commercially available printer. For the metallic mesh sensor printed with 500 pg/mm² (11 fmol) horseradish peroxidase, a red-shift of the the transmission dip frequency is observed clearly, which is based on the variation of the refractive index in the vicinity of the metallic mesh openings. This result exceeds the detection limit of conventional THz spectroscopy for protein molecules. Next we have successfully demonstrated a label-free detection of streptavidin-biotin interaction on a PVDF membrane. The streptavidin-biotin interaction can be detected by using 650 pg/mm² (2.5 pmol) biotin. These results indicates that our sensing system has high sensitivity and we have successfully demonstrated a convenient system by using a metallic mesh and PVDF membrane. As a next challenge, we aim to achieve a label-free selective detection of proteins by using an antigen/antibody reaction.

ACKNOWLEDGEMENTS

This work was supported in part by a Grant-in-Aid for Young Scientists (18070501) from The Ministry of Health, Labour and Welfare of Japan.

REFERENCES

1. R. Ulrich, *Infrared Physics*, **7**, 37 (1967).
2. K. Sakai, T. Fukui, Y. Tsunawaki, and H. Yoshinaga, *Jpn. J. Appl. Phys.*, **8**, 1046 (1969).
3. H. Raether, *Surface Plasmons on Smooth and Rough Surfaces and on Gratings* (Springer-Verlag, Berlin, 1988).
4. F. Miyamaru and M. Hangyo, *Appl. Phys. Lett.*, **84**, 2742 (2004).
5. H. Cao and A. Nahata, *Opt. Exp.*, **12**, 1004 (2004).
6. F. Miyamaru, S. Hayashi, C. Otani, K. Kawase, Y. Ogawa, H. Yoshida, and E. Kato, *Opt. Lett.*, **31**, 1118 (2006).
7. L. Martin-Moreno, F. J. Garcia-Vidal, H. J. Lezec, K. M. Pellerin, T. Thio, J. B. Pendry, and T. W. Ebbesen, *Phys. Rev. Lett.*, **86**, 1114 (2001).
8. E. Popov, M. Neviere, S. Enoch and R. Reinisch, *Phys. Rev. B*, **62**, 16100 (2000).
9. H. F. Ghaemi, T. Thio, D. E. Grupp, T. W. Ebbesen, and H. J. Lezec, *Phys. Rev. B.*, **58**, 6779 (1998).
10. T. Okamoto, T. Suzuki and N. Yamamoto, *Nature Biotech.*, **18**, 438 (2000).

Terahertz Sensing for Ensuring the Safety and Security

Y. Ogawa¹, S. Hayashi^{1,2}, C. Otani², and K. Kawase^{1,2,3}

¹Tohoku University, Japan

²RIKEN, Japan

³Nagoya University, Japan

Abstract— We are studying some novel steps toward real-life applications of terahertz wave. In this paper, we introduce two THz sensing methods for ensuring the safety and security of the lives of people, such as, i) Nondestructive detection of illicit drugs using spectral fingerprints, ii) Label-free detections of protein-protein interactions for allergy test.

1. INTRODUCTION

Terahertz (THz) waves, at the gap between microwaves and the far infrared, have long been unexplored field, mainly because of the lack of sources and detectors. However, recent remarkable developments in THz technology allow THz radiation to be applied in solving real-world problems, such as in material science, atmospheric research, biology, solid state physics, chemistry and gas tracing [1,2]. Among the most prominent advantages that the THz radiation offers we mention its ability to penetrate a wide range of materials which are opaque to visible and near infrared light or produce only low-contrast X-ray images. As the THz photon energy is roughly six orders of magnitude smaller than that of an X-ray photon, its interaction with matter, particularly with biological tissues, is considered to cause no detectable damage, at least not by ionization processes. A comparison with the other side of the electromagnetic spectrum, the microwave range, highlights again the advantage of THz waves: With their shorter wavelength they provide a considerably better imaging resolution that is sufficient in many applications. The existence of chemically-specific absorption spectra in the THz range, reflecting molecular transitions and intermolecular bonds, facilitates fingerprinting and brings about a whole area of spectroscopic detection, testing, and analysis techniques. On the other hand, the technologies for ensuring the safety and security have been becoming the important in an increasingly internationalized world. The THz technology has been expected to solve such problems. We have been studying a few THz sensing methods for ensuring the safety and security of the lives of people, such as, i) Nondestructive detection of illicit drugs using spectral fingerprints, ii) Label-free detections of protein-protein interactions for allergy test.

The absence of non-destructive inspection technique for illicit drugs hidden in mail envelopes has resulted in such drugs being not only smuggled across international borders but also transported from one jurisdiction to another within a country with surprising ease. The situation must also be attributed to the inconvenience of having to obtain a search warrant to examine the contents every time the need arises. A majority of the legal systems in the world prohibit private letters, whether they are suspected or otherwise, from being examined without a search warrant. There exist several inspection techniques such as passing the mail through an X-ray scanner, having it sniffed by a trained dog, or swiping its outside with a trace detection system. However, the ability of X-ray scanners is limited to identifying the shape of a vinyl plastic bag or a tablet, and not the type of the drug, providing insufficient grounds for opening the envelope for examination. Trace detection and canine detection, on the other hand, can only be effective if there are detectable signs outside the envelope, such as a scent or trace amounts of the concealed drug. In contrast, the THz-wave is suitable for drug detection purposes, being able to screen the contents of envelopes and our measurement results having proven the existence of fingerprint spectra peculiar to illicit drugs in the THz region. In this paper, we will report a demonstration to detect illicit drugs in envelope using a THz spectroscopic imaging system.

In recent years, Japanese consumers have become increasingly aware of food safety issues (e.g., residual agricultural chemicals in food, mislabeled beef and tampered food). In particular, a detection of an allergic substance in food materials is very important, because a substance that triggers allergies causes serious allergic reaction. We think the label-free biosensing is a good way to detect them. However, it is necessary to detect a very small amount of allergen in food. To obtain high sensitivity, we demonstrated a sensing application using thin metallic mesh — a two-dimensional array of sub-wavelength holes.

2. NONDESTRUCTIVE DETECTION OF ILLICIT DRUGS USING SPECTRAL FINGERPRINTS [3]

We have developed a basic technology for terahertz imaging, which allows detection and identification of drugs concealed in envelopes, by introducing the component spatial pattern analysis [4]. As samples we chose for this experiment three drugs that were: methamphetamine (*d*-methamphetamine hydrochloride, more than 98% purity), currently the most widely consumed drug of abuse in Japan, MDMA (*dl*-3, 4-methylenedioxyamphetamine hydrochloride, 67% purity), another drug of abuse becoming widespread on a global scale, and aspirin (100% purity) as a reference. As shown in Fig. 1, ~20mg of each substance were placed in a small 10 × 10mm polyethylene bag. The three bags were then placed inside a usual airmail-type envelope. THz images of the rectangular area indicated by the white line in Fig. 1 were captured.

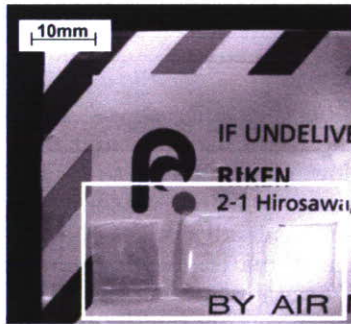


Figure 1: View of the samples. The small polyethylene bags contain from left to right: MDMA, aspirin, and methamphetamine. The bags were placed inside the envelope during imaging. The area indicated by the white line represents the imaging target, 20 × 38 mm in size. Since methamphetamine and aspirin are similar in appearance, we used a slightly longer bag for the latter to avoid confusion.

The THz spectroscopic imaging system [5] consists of a Q-switched Nd:YAG laser, a TPO (THz-wave parametric oscillator) [6], imaging optics, an *xy* scanning stage, a detector, a lock-in amplifier, and a personal computer. By changing the frequency emitted by the TPO within the 1.3 to 2.0 THz range, we obtained seven multispectral images as shown in Fig. 2. In Fig. 2, the scale of the image $-\ln(I_t/I_0)$ is the logarithm of the transmitted THz-wave intensity I_t divided by the intensity of the THz-wave that was only transmitted through the envelope I_0 . This means that the greater the absorption, the brighter the shades.

The absorption spectra of the three drugs were measured with the same TPO system as shown in Fig. 3. The corresponding absorption intensity values at the seven frequencies were extracted to obtain the information of spectra. Although the spectra of methamphetamine and MDMA are

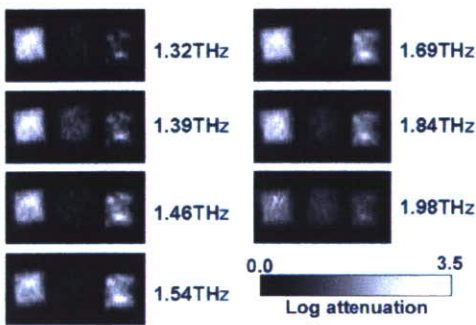


Figure 2: Seven multispectral images.

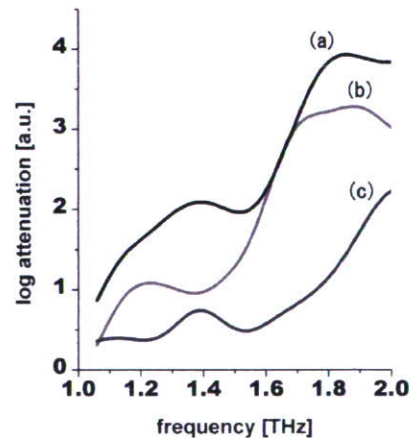


Figure 3: Absorption spectra of MDMA (a), methamphetamine (b), and aspirin (c).

similar, the difference between them enabled us to distinguish between the two using the component pattern analysis method.

By using the seven recorded images and the information of spectra, the spatial pattern was calculated. Fig. 4 shows the result of extracting the three components, with each image corresponding to each of the sample drugs. As it is evident from these images, the three drugs have been clearly distinguished and the corresponding spatial patterns obtained. A ROI (region of interest) was set in each area of the component patterns in Fig. 4 and then we took the average of tone in each ROI. The ROI was a square with 20×20 pixels, which is similar to the size of a plastic bag. The averages of MDMA, aspirin, and methamphetamine were 122, 119 and 138, respectively. The errors were less than $\pm 10\%$, which is sufficient for the drug detection purposes.

3. LABEL-FREE DETECTION OF PROTEIN-PROTEIN INTERACTIONS FOR ALLERGY TEST

We have been developing a novel sensing method which uses the high-sensitivity phenomenon of a thin conductive metal mesh. The transmission characteristics of thin metallic meshes, investigated since the 1960s [7, 8], are those of a band-pass filter in the far-infrared region. The transmission properties of a thin metallic mesh are determined mainly by its geometric parameters, but, when a material is placed near the mesh openings, are also affected by the refractive index of that material, in the sense that a shift of the resonant transmission frequency occurs [9]. Our sensing method is based on the change of the transmittance of THz radiation through a thin metallic mesh accompanied by the resonant frequency shift when a sample substance is applied on the mesh openings. The transmittance of the thin metallic mesh does not change due to the absorption, but dominantly due to the variation of the refractive index of the sample substances near the openings [10].

In our experiment, we measured the transmission spectra of a thin metallic mesh using a Fourier Transform Infrared (FT-IR) spectrometer, in which the THz beam was focused into an area of about 7 mm in diameter on the thin metallic mesh. The transmission dip frequency shows the incident angle dependence [11]. We observed the shift of this transmission dip frequency. The thin metallic mesh was made from electroformed nickel, allowing the fabrication of a smooth surface and precise periodicity of the grating. The two dimensional square metallic mesh was $6 \mu\text{m}$ thick with a grating period of $76.3 \mu\text{m}$ and a metallic line width of $18.3 \mu\text{m}$, in both dimensions. This metallic mesh behaves as a high-pass filter and the transmission at the dip frequency is approximately 70% at 2.94 THz (Fig. 5).

We demonstrate the experiment of a label-free detection of casein/anti-casein reaction which causes allergy to milk. We used alpha-casein from bobime milk and rabbit IgG anti alpha-casein. For quantitative blotting the antigen protein (alpha-casein) to a polyvinylidene difluoride (PVDF)

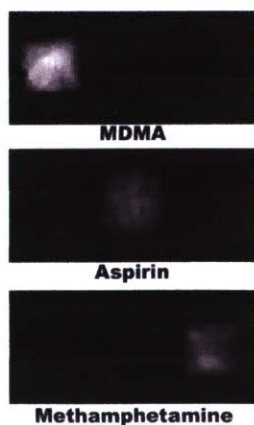


Figure 4: Extracted spatial patterns of MDMA, aspirin and methamphetamine, using the component spatial pattern analysis. The three drugs are clearly distinguished and corresponding spatial patterns obtained.

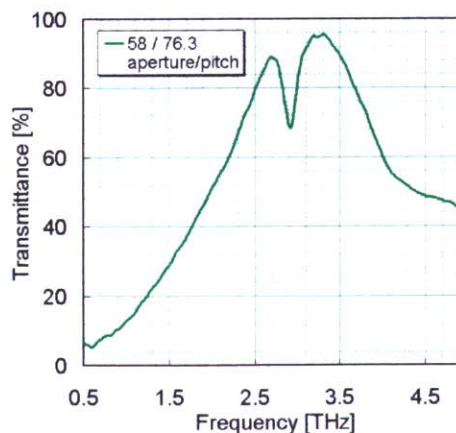


Figure 5: A measured transmission spectrum of the thin metal mesh. This metal mesh behaves as a high-pass filter and the peak transmission is approximately 95% at 3.37 THz. The transmittance of dip is observed at 2.94 THz.

membrane, we used a printing device (KONICA MINOLTA IJ co., Japan). The amount of the sample was controlled using an image processing software. For viscosity control, alpha-casein was dissolved in solution of glycerine (40%) and isopropyl alcohol (5%) in distilled water. In our case, the solution concentration is 1.0 mg/ml. In order to make the PVDF membrane hydrophilic it was soaked in methanol 100% for 20 seconds, then washed with distilled water for 2×5 minutes and rinsed in Tris-buffered saline (TBS) (20 mM Tris, 500 mM NaCl, pH 7.5). Alpha-casein solution was applied by the printing device on the membrane. The blotted membrane was immersed in the blocking with the BSA solution (0.1% BSA in TTBS (20 mM Tris, 500 mM NaCl, 0.05% Tween-20, pH 7.5)) for 2 hours at room temperature. After the washing with the TTBS solution, it was incubated with 20 μ l monoclonal rabbit IgG anti alpha-casein (1.0 mg/ml) over night at room temperature.

We measured samples using our FT-IR at three steps PVDF membrane which were (a) untreated, (b) applied alpha-casein solution and blocked with the BSA solution, and (c) incubated with rabbit IgG anti alpha-casein. The PVDF membrane shows transmittance more than 70% under 3 THz. Each PVDF membrane was attached to the input surface of the thin metallic mesh. We present the transmission spectra only in the frequency range around the transmission dip observed in Fig. 6. The transmission dip frequency, which is estimated from the fitting of the measured spectrum with a Lorentz function, is plotted in the inset of Fig. 6 as a function of each step. The transmission spectrum of the applied-casein solution and blocked with the BSA solution on PVDF membrane (b) was found to shift towards lower frequencies relative to the untreated PVDF membrane (a). And the transmission spectrum of the incubated with rabbit IgG anti alpha-casein on PVDF membrane (c) was also found to shift towards lower frequencies relative to the non-incubated PVDF membrane (b). In this case, the amount of rabbit IgG anti alpha-casein on PVDF membrane is estimated 8.7×10^{-7} M. This shift is believed to be caused by the different refractive index of antigen-antibody combination in the vicinity of metallic mesh. Such a small variation of the transmittance makes it difficult to detect the sample substances by monitoring the transmission intensity at a single frequency. However, owing to the shift of the dip frequency depending on the refractive index in the vicinity of the metallic openings, a sensitive detection of the sample substances becomes possible with the single frequency source in the THz regime.

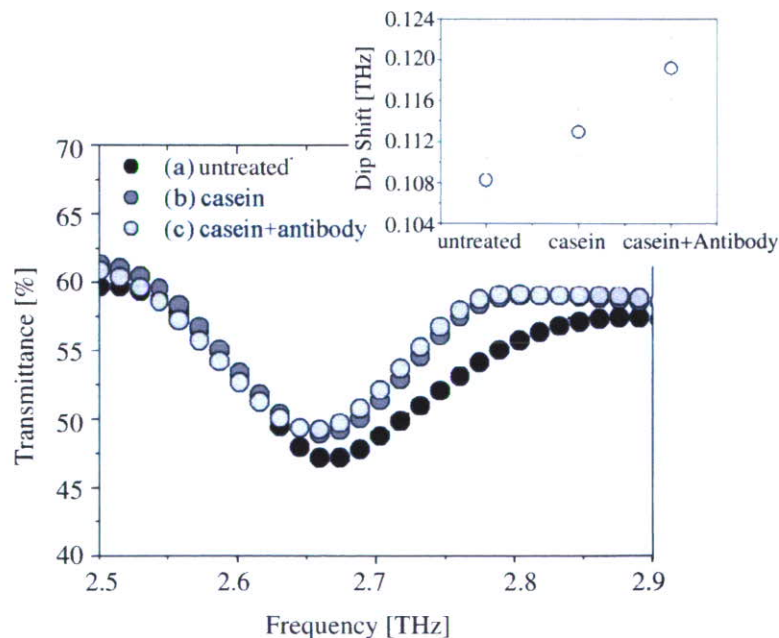


Figure 6: Measured transmission spectra of a thin metallic mesh with various conditions of PVDF membrane. At the inset figure shows the shift of transmission dip frequency as a function of the each conditions of PVDF membrane.

ACKNOWLEDGMENT

This work was supported in part by a Grant-in-Aid for Young Scientists from The Ministry of Health, Labour and Welfare of Japan.

REFERENCES

1. Tonouchi, M., "Cutting-edge terahertz technology," *Nature Photonics*, Vol. 1, 97–105, 2007.
2. Ferguson, B. and X.-C. Zhang, "Materials for terahertz science and technology," *Nature Materials*, Vol. 1, 26–33, 2002.
3. Kawase, K., Y. Ogawa, Y. Watanabe, and H. Inoue, "Non-destructive terahertz imaging of illicit drugs using spectral fingerprints," *Opt. Express*, Vol. 11, 2549–2554, 2003.
4. Kawata, S., K. Sasaki, and S. Minami, "Component analysis of spatial and spectral patterns in multispectral images. I. Basis.," *J. Opt. Soc. Am. A*, Vol. 4, 2101–2106, 1987.
5. Watanabe, Y., K. Kawase, T. Ikari, H. Ito, Y. Ishikawa, and H. Minamide, "Component spatial pattern analysis of chemicals using terahertz spectroscopic imaging," *Appl. Phys. Lett.*, Vol. 83, 800–802, 2003.
6. Kawase, K., J. Shikata, and H. Ito, "Terahertz wave parametric source," *J. Phys. D: Appl. Phys.*, Vol. 35, R1–R14, 2002.
7. Ulrich, R., "Far-infrared properties of metallic mesh and its complimentary structure," *Infrared Phys.*, Vol. 7, 37–55, 1967.
8. Sakai, K., T. Fukui, Y. Tsunawaki, and H. Yoshinaga, "Metallic mesh bandpass filters and fabry-perot interferometer for the far infrared," *Jpn. J. Appl. Phys.*, Vol. 8, 1046–1055, 1969.
9. Miyamaru, F. and M. Hangyo, "Finite size effect of transmission property for metal hole arrays in subterahertz region," *Appl. Phys. Lett.*, Vol. 84, 2742–2744, 2004.
10. Miyamaru, F., S. Hayashi, C. Otani, K. Kawase, Y. Ogawa, H. Yoshida, and E. Kato, "Terahertz surface-wave resonant sensor with a metal hole array," *Opt. Lett.*, Vol. 31, 1118–1120, 2006.
11. Lamarre, J. M., N. Coron, R. Courtin, G. Dambier, and M. Charra, "Metallic mesh properties and design of submillimeter filters," *Int. J. of Infrared and Millimeter Waves*, Vol. 2, 273–292, 1981.

【第5講】

食の安全・安心のためのテラヘルツ波応用に関する研究

小川雄一

東北大学大学院農学研究科

1. はじめに

近年、O-157などの病原性細菌による食中毒問題や、未登録農薬の違法使用発覚、牛肉問題に端を発する偽装表示問題などの事件が消費者に不安を与えている。このように農産物および食品の安全性や品質についての信頼性が揺らぐ問題が発生し、消費者からは安全性の証明を求める動きが活発化している。そのため、国内外の食品や農産物に対して様々な検査や分析が必要となり、X線や近赤外、マイクロ波など多くの電磁波が利用されている。

一方、現在世界中でテラヘルツ(THz)波の応用研究が盛んに行われ、光源開発など新しい技術開発以外にも、数多くの応用可能性が報告されている。その中でも特に、先の電磁波同様、THz波ならではの利用法が見出されつつあり、その応用開拓の動向に注目が向けられている。例えば、THz帯の分光スペクトルは多くの物質で既に見出されており、赤外域とは異なる利用方法が期待されている。これらの情報を使った結晶多形や半導体の評価は、その代表的な応用例^{1) 3)}といえる。また、最近では生体高分子をターゲットとした研究も注目されている。生体高分子の高次構造の形成に起因する吸収がTHz帯に存在するため、蛍光標識を用いることなくDNAのハイブリダイゼーションや抗原抗体反応をセンシングできるため、生体高分子などのラベルフリーセンシングに関する研究が報告されている^{4) 7)}。

我々は、THz波の特性を利用し、食の安全・安心のための応用研究を行っている。本稿では特に、食品の品質を検査するための技術と、牛海綿状脳症(BSE)や残留農薬検査などへの応用を目指したタンパク質分析技術について述べる。THz帯は水の吸収係数が高い(約 200 cm^{-1} @1 THz)ことが知られており⁸⁾、このことを積極的に利用することで、高感度な水分計測が可能となる。そこで一般に広く食品分析に利用されているカールフィッシャー法との比較を行い、THz波による簡便な食品中水分計測の可能性を検討した。また、チーズの品質管理を目指し、THz帯の分光スペクトルとケルダール法など従来の成分分析法との比較を行った。さらに、食の安全を確保するためのタンパク質などの生体高分子の分析は、微量な分析が必要となることが多い。そこで、金属メッシュを利用した高感度分析法の検討を試みた。

2. 食品の品質評価への応用

2.1 食品油中の水分計測

食品中の水は、食品の品質や味、貯蔵、酵素活性、

微生物の成長などに影響を与える⁹⁾ため、食品中の水分を測定することは重要な意味を持つことから現在までに様々な水分計測法が確立されている。また、食用油中の水分は加水分解の原因となるため¹⁰⁾、日本農林規格(JAS)により水分量は0.3%以下であることが定められており、JASは公定法としてカールフィッシャー法を定めている¹¹⁾。本手法は滴定フラスコ内で試料を脱水溶剤に溶解し、試料中の水分を抽出した後、ヨウ素、二酸化硫黄、塩基を主成分としたカールフィッシャー試薬(滴定溶剤)で滴定することにより水分量を求める方法である。このため、分析には有機溶剤を用いた抜き取り検査が必要となる。一方、THz帯において、油は水よりも高い透過性を示す。そこで微量な水分を含む食用油について、遠赤外用のフーリエ変換式赤外分光光度計(以下、FT-IR)を用いて透過測定を行い、既存のカールフィッシャー法とTHz帯の吸光度との相関を調べた。その実験結果を図1に示す。

本実験は光路長が1 mmの石英セルを用いて透過測定を行っており、検量線の作成には、1.5 THzでの吸光度を用いている。この結果、JASにより定められている0.3%以下の水分量においても相関が認められる。本技術は従来の有機溶剤や抜き取り検査を不要とし、容器越しの測定が可能であることから、今後品質管理のための食用油脂中の水分計測での応用が考えられる。

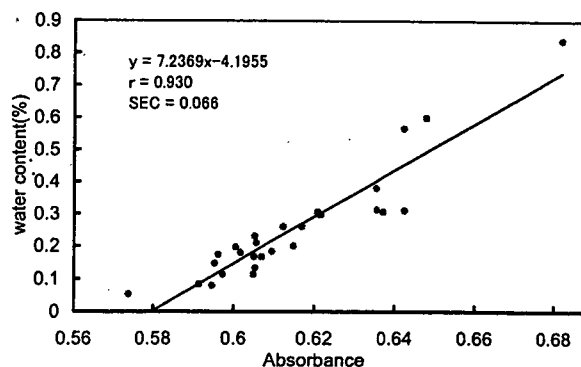


図1 カールフィッシャー法による分析結果と吸光度(@ 50 cm^{-1})の相関

2.2 糖結晶中の水和水計測

食品や医薬品の中に含まれる僅かな水は、様々な状態で相互に影響を与えることが知られている。そのひとつが水和水と呼ばれる結合状態である。水和水の要因としては、静電的相互作用、水素結合、ファンデルワールス力や疎水性水和水などがある¹²⁾。疎水性アミノ酸の水和水は、タンパク質の安定性に大きな影響を与えていると言

われている¹³⁾⁻¹⁵⁾。また食品に関しては品質を管理する上で水と水量を計測する製品などが市販されている。一方医薬品分野では結晶多形をとる医薬品が数多く存在している¹⁶⁾。結晶多形をとる物質は水和物になりやすく¹⁷⁾、医薬品に結合した水分により、溶解性、吸収性、生理活性が異なる¹⁸⁾⁻²⁰⁾。このため、水和を防ぐための数々の賦形剤が使用されている²¹⁾。

そこで本研究では、物質の安定性や溶解性に重要な役割を担っている粉体中の水分量を知る分析方法として、THz 分光スペクトルを利用し、モデルとしてグルコースをホワイトポリエチレンで希釈したペレットを使用し、定量的な分析を試みた。グルコース粉末は、水和物と無水物の状態で存在し、これらの違いは分子間相互作用の違いとして表れることが期待できる。そこでカルフィッシャー法による水分計測結果と THz 帯分光スペクトルの関係について調べた。なお、THz 帯の分光測定には先の実験と同じ FT-IR を使用した。

図2に一水和物から無水物に変化するグルコースの吸光度スペクトルを示す。これらのサンプルは、カルフィッシャー法で水分含量を測定した結果、重量パーセントで 8.77 % (一水和物)、6.31 % (脱水和物 1)、2.45 % (脱水和物 2)、1.52 % (脱水和物 3)、0.15 % (無水物)であった。この帯域では、水のみ分光スペクトルには特徴的な吸収ピークが見られず、ブロードなスペクトルを示すため、これらの明瞭な吸収ピークは水分子とグルコースの相互作用に起因するものと推測できる。

吸収ピークは、一水和物の場合、60.3 cm^{-1} 、65.6 cm^{-1} 、80.5 cm^{-1} に表れ、無水物では、47.7 cm^{-1} 、69.4 cm^{-1} 、89.1 cm^{-1} 、98.3 cm^{-1} に表れている。脱水和物の場合、一水和物と無水物の両方のスペクトルの特徴を併せ持つが、水分量が少なくなるにつれて、一水和物に特徴的な 47.7 cm^{-1} 、80.5 cm^{-1} の吸収ピークが減少し、無水物に特徴的な 69.4 cm^{-1} 、89.1 cm^{-1} 、98.3 cm^{-1} のピークが増加していく様子が観測された。このような水分の減少に伴う明瞭なスペクトル形状の変化が観察されたのは、加熱による水の脱離により水和物の分子全体の大きな振動モードや水素結合などの分子間の相互作用、フォノンモードが変化したためと考えられる²²⁾⁻²⁴⁾。この結果から、THz 帯で見られる分光スペクトルの変化は、グルコース分子内の水と水による影響によるものである

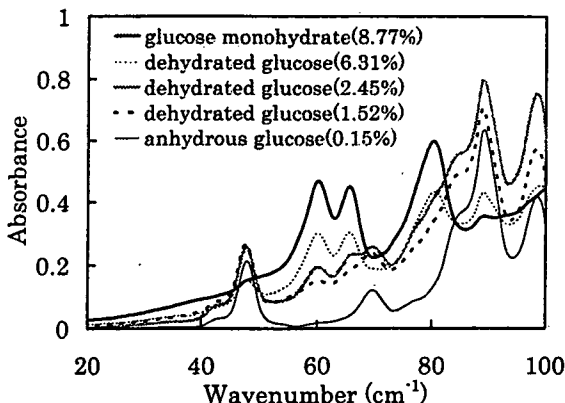


図2 水分量の異なるグルコース結晶のスペクトル

と考えられる。

さらに吸収ピークの詳細な分析を行い、水分量と重相関の高い周波数の組み合わせを求め、その検量線の評価を行った。その結果、最も低い予測標準誤差 (SEP) が得られるものは 60.3 cm^{-1} 、65.6 cm^{-1} 、80.5 cm^{-1} の波数を用いて検量線を作成したものであり、重相関係数(R)は 0.9521、予測標準誤差(SEP)は 0.736 であった。図3に評価用試料を用いて評価したときの試料散布図を示す。

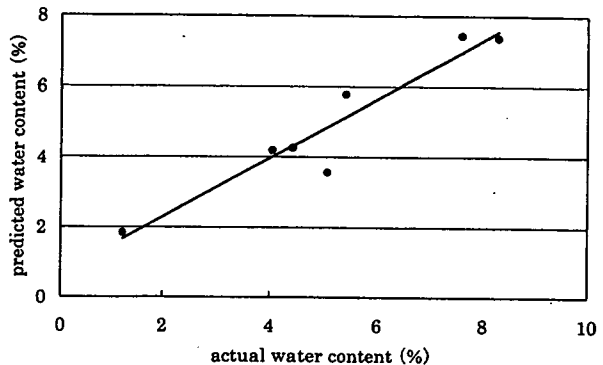


図3 予測値と実測値の検量線評価結果

($R = 0.9521$, $SEP = 0.736$)

Houghらのグルコース一水和物結晶に関する報告²⁵⁾から、グルコース一水和物結晶の水分子は、4つのグルコース分子に水素結合によって捕らえられていることが考えられる。この条件のもと、一分子モデルでの量子計算(B3LYP/6-31G(d,p), B3LYP/6-311++G(d,p))を行った結果、c-c結合の周りの内部よじれ振動が、主に今回の実験結果でスペクトルが大きく変化した 60.3、65.6、80.5 cm^{-1} に表れ、このうち、65.6 cm^{-1} は等価な2つの振動であることがわかった。また、最も水分子が抜けやすいと考えられるのは、キャビティーの大きいb軸と考えられる。このb軸から優先して抜けた場合、4つのグルコースと順次水素結合(そのうち2つは等価な振動)が脱離し、相互作用の変化がTHz帯分光スペクトルに表れると考えられる。このことから、本研究で見られたTHz帯分光スペクトルの変化は、水の脱離に伴う分子間相互作用の変化を反映したものと考えられる。

2.3 チーズの分光測定

近年の生産規模の拡大と食の安全に対する意識向上を背景として、より迅速な検査への需要が高まっている。このことを受け、簡便で試薬を必要としない赤外・近赤外領域の電磁波を利用した分析手法が研究されてきた。この方法は分子内結合を観測するもので、生乳の成分分析では米国の公定法として認められているなど既に実用化がなされている。チーズは欧米では一般的な食材であり、品質評価に関しても幅広く研究が進められている²⁶⁾⁻²⁸⁾。主成分である水分、タンパク質、脂質はTHz領域ではそれぞれ吸収の度合いが異なる。また、チーズには脂肪球のような数十 μm 程度からカゼインミ